Mechanics & Industry **26**, 35 (2025)
© B. Chen et al., Published by EDP Sciences 2025
https://doi.org/10.1051/meca/2025017

Mechanics & Industry

Available online at:
www.mechanics-industry.org

Original Article

Open Access

Agricultural tractors magneto-rheological seat suspension design based on LADRC control strategy

Bin Chen[1,2,3], Bo Guo[1,2,3,*], Luyang Zhou[2,3], Zhixiong Zheng[2,3], Jianjin Wu[2,3], and Minghao Duan[2,3]

[1] Fujian Key Laboratory of Big Data Application and Intellectualization for Tea Industry, Wuyi University, Nanping, Fujian 354300, PR China
[2] The Key Laboratory for Agricultural Machinery Intelligent Control and Manufacturing of Fujian Education Institutions, Wuyi University, Nanping, Fujian 354300, PR China
[3] Fujian Provincial University Research Center for Digitalization and Intellectualization of the Bamboo Whole Industry Chain, Wuyi University, Nanping, Fujian 354300, PR China

Received: 7 September 2024 / Accepted: 10 July 2025

Abstract. This paper proposes a novel semi-active suspension control method for agricultural tractor seats based on Linear Active Disturbance Rejection Control (LADRC). A two-degree-of-freedom magnetorheological (MR) seat suspension dynamic model was developed, and the Bouc-Wen model was adopted for nonlinear modeling and validation of the damper, based on experimental data of MR damper mechanical performance. The LADRC strategy was innovatively applied to the seat suspension system and validated through simulation in the MATLAB environment. The results indicate that the LADRC strategy significantly reduced vertical vibration acceleration. Compared to traditional PID control, under D-level random and impact road surface excitations, when the agricultural tractor speed is 1 m/s, the seat vertical acceleration decreased by 15.0% and 24.2%, respectively, and the root mean square (RMS) acceleration was controlled within 0.70. When the agricultural tractor speed increased to 2 m/s, the reductions reached 18.7% and 29.5%, respectively, and the RMS value was controlled within 0.75, significantly improving the operational comfort and vibration isolation performance of agricultural tractor.

Keywords: LADRC / agricultural tractor / nonlinear control / Bouc-Wen model / LADRC / vibration isolation

1 Introduction

As agricultural modernization progresses, agricultural tractors, which are key equipment for enhancing agricultural productivity, are increasingly focused on by users for their driving comfort and operational convenience. The suspension systems of traditional agricultural tractors frequently employ passive vibration damping designs with fixed stiffness and damping coefficients. While these designs may provide basic vibration reduction under certain conditions, they often fail to meet users' higher expectations for comfort in diverse agricultural operations. In comparison to passive suspension systems, semi-active seat suspensions exhibit notable advantages in terms of cost control and structural simplification, while simultaneously offering superior vibration damping performance [1–3]. Although active suspension systems may offer superior damping effects, their high cost and complex design may not be practical for agricultural equipment like tractors, which are designed to be cost-effective. Consequently, the development of cost-effective and efficient semi-active seat suspension systems tailored to the specific operational requirements of agricultural tractors has become a crucial research direction with the objective of enhancing their driving comfort. MR control technology represents an emerging high-end vibration damping method that allows for precise control of MR dampers with simple control strategies and minimal energy input. For agricultural machinery such as tractors that operate at low speeds in complex and variable farmland environments, the use of appropriately structured and strategically controlled MR dampers for seat vibration reduction has been demonstrated to have significant effects and to offer high cost-effectiveness. Consequently, the application of MR technology to semi-active seat suspensions in agricultural tractors not only offers considerable research potential but also possesses significant practical value [4–6].

MR semi-active suspensions, known for their simple structure, quick response, low energy consumption, and adjustable damping force, have broad application

* e-mail: iamguobo@wuyiu.edu.cn

This is an Open Access article distributed under the terms of the Creative Commons Attribution License (https://creativecommons.org/licenses/by/4.0), which permits unrestricted use, distribution, and reproduction in any medium, provided the original work is properly cited.

prospects in vehicle suspensions and seat mounts, becoming a focus of research and interest. Currently, there is extensive research on control strategies for MR semi-active suspensions, involving various methods such as PID control, fuzzy control, skyhook control, model predictive control (MPC), and sliding mode control (SMC). Gheibollahi, H. et al. addressed the problem of articulated semi-trailer ride comfort optimization by investigating and proposing a coupled system combining a 13-degree-of-freedom truck model with a 4-degree-of-freedom bio-dynamic model and designing two active seat suspension controllers, Genetic Algorithm (GA)-PID and Fuzzy PID. The two controllers aim to reduce the comprehensive comfort indexes such as motion sickness dose value (37.42%), vibration dose value (37.53%), and whole-body RMS acceleration (37.40%), and optimize the PID parameters globally by GA, and dynamically regulate the control rules by combining fuzzy logic. The simulation results show that compared with the passive suspension, the two controllers are effective in suppressing the vibration energy (39.51% reduction in peak value) and alleviating the human physiological discomfort (14.41% reduction in excessive kurtosis), which verifies the universality and co-optimization potential of the intelligent algorithms in multi-degree-of-freedom vehicle systems [7]. Sunil Kumar Sharma and colleagues integrated MR dampers into marine diesel engine systems and developed a fuzzy logic self-tuning PID controller, establishing a semi-active isolator. Experimental validations demonstrated that the vibration damping characteristics of the MR-based fuzzy logic self-tuning PID controller were significantly enhanced, especially under various operating conditions [8]. Gheibollahi, H. et al. In order to balance the ride comfort and control energy consumption of articulated truck seat suspension, the study constructs a 13-degree-of-freedom linear truck model with seat RMS acceleration (comfort metrics) and controller RMS force (energy consumption metrics) as multi-objective optimization functions. Based on the NSGA-II algorithm to generate the Pareto frontier, the optimal parameters are screened by combining with TOPSIS, and the effects of trailer load, tire stiffness and other parameters are evaluated by Monte Carlo sensitivity analysis. The experiments show that the optimization improves the comfort by 25% at class C road (60 km/h) and reduces the control force by 60% at the same speed at class A road; the ISO 2631-1 standard validation shows that the two indexes are significantly optimized and the validity of the results is confirmed by MSC-ADAMS simulation. This study provides an energy-performance co-optimization paradigm for multi-objective active suspension design [9]. Najafi, A. et al. proposed a multidimensional fuzzy sliding controller (TFSMC) based on genetic algorithm optimization for dynamic performance optimization of active variable geometry suspension. By constructing a dual-input Mamdani fuzzy controller that integrates vehicle roll, pitch angle acceleration and vertical acceleration, combined with triple fuzzy sliding modes and dynamic optimization strategy of sliding surface parameters, the body vibration (roll/pitch angle acceleration reduction) and tire deflection (up to 15% reduction) are effectively suppressed, and the lateral stability and ride comfort are simultaneously improved. Experimental validation shows that the TFSMC performs optimally under 53% and 73% of the test conditions in on-road and off-road scenarios, respectively, with a 30% improvement in lateral stability and a 10% reduction in body rebound acceleration compared with the passive system, and further reduces the chattering effect through the optimization of sliding surface parameters by genetic algorithms, which provides a multi-objective synergistic control solution for the suspension system under complex road conditions [10]. Damavandi, A. D. et al. analyzed the dynamic performance by screening 24 symmetrical structures among 180 hydraulic interconnected suspension configurations, constructing a 14-degree-of-freedom vehicle model, and optimizing six hydraulic parameters using a genetic algorithm. The results show that the optimized four configurations reduce the maximum body rebound acceleration by 47% (27% on average) and the pitch angle response by 18% in random road tests; the lateral inclination angle reduction under the side wind condition reaches 18%, and the roll angle synchronization is reduced by 3%. Multi-scenario verification shows that the optimized configuration achieves a balance between ride smoothness and handling stability through parameter synergistic tuning, highlighting the multi-objective optimization potential and dynamic adaptability of hydraulic interconnected suspension under complex working conditions [11]. Jayu Kim et al. proposed a Model Predictive Control (MPC) method for semi-active suspensions that optimizes ride comfort and handling performance by previewing road information and compensating for shift delays. They used a model-based Kalman filter to estimate the suspension state and considered mechanical constraints to determine the feasible region for control inputs. To address computational load and shift time delay issues, they introduced a model predictive system that incorporates the full vehicle dynamics model and road preview information. The effectiveness of the algorithm was validated through computer simulations, and it was successfully applied in real vehicle tests, significantly enhancing ride comfort [12]. Gang Li et al. developed a semi-active air suspension fuzzy sliding mode control strategy (FSMC) based on MR dampers. By testing MR dampers and optimizing the hyperbolic tangent model parameters using genetic algorithms, the researchers established an inverse model of the MR damper. The implementation of fuzzy control within the sliding mode control boundary layer resulted in a notable enhancement in system stability and control precision [13]. Recent studies have focused on various control strategies for semi-active suspension systems, such as PID control and MPC. However, while these methods offer effective vibration reduction, they often require complex parameter tuning or are computationally intensive. In contrast, the LADRC strategy presented in this study provides a simpler, more computationally efficient solution, which is particularly suitable for real-time control in agricultural tractors.

In summary, semi-active seat suspensions with MR dampers offer excellent vibration damping performance compared to conventional passive suspension systems, while maintaining cost control and structural simplicity. Advanced

control strategies such as MPC and FSMC have been explored, but they typically require complex tuning and may not be applicable to the dynamic and nonlinear characteristics of agricultural tractor seat suspensions. Improving the comfort of agricultural tractor seat suspensions not only improves operator comfort, but also reduces fatigue, thereby increasing productivity. This is particularly important in the developing agricultural sector where long hours of operation are prevalent. The nonlinear dynamics and time-varying and lag characteristics of MR dampers present significant challenges in accurately modeling them. Although various control strategies exist, there is still room for improvement in their design, especially in terms of enhancing algorithm efficiency and controller performance [14–18]. To enhance the vibration damping performance of MR dampers in seat suspensions, a novel LADRC strategy is introduced. LADRC is renowned for its resilience to variations in system parameters and external disturbances, and its ability to function effectively in the presence of imperfections in the system model. It is particularly adept at adapting to changes in system dynamics and excels in the management of complex and nonlinear seat vibration systems. In comparison with the aforementioned control strategies, such as fuzzy-PID, GA-PID, SMC, and MPC, LADRC exhibits several notable advantages. These include the capacity for straightforward parameter adjustment, minimal computing power requirements, and relatively low complexity. This renders it particularly wellsuited for the vibration isolation control of agricultural tractor seats. Additionally, its implementation can result in a reduction in the cost of practical applications to a considerable extent.

In this paper, a semi-active control method is proposed for the characterization of MR dampers and the operation of seat suspensions for agricultural machinery. This involves the development of a two-degree-of-freedom seat suspension model containing an MR fluid damper and a stochastic road excitation model. The designed MR damper is nonlinearly modeled using a Bouc-Wen model based on the results of mechanical performance tests of the MR damper. In the dynamic modeling of the seat MR damper, LADRC is applied to the seat suspension for the first time. Simulations and practical tests demonstrate the effectiveness of the continuously adjustable MR damped seat suspension, which is effectively controlled by applying LADRC and Bouc-Wen model. The control strategy not only improves operator comfort but also reduces fatigue, leading to increased productivity and improved comfort in agricultural tractor seat suspensions. This is particularly important in the developing agricultural sector where long hours of operation are common.

2 Seat suspension dynamics model

The two-degree-of-freedom dynamic model of the MR damper seat suspension system is shown in Figure 1. In the figure, $\boldsymbol{m_1}$ and $\boldsymbol{m_s}$ denote the mass of the human body and the seat, respectively; $\boldsymbol{k_1}$ and $\boldsymbol{c_1}$ denote the stiffness and damping of the human body, respectively; $\boldsymbol{k_s}$ and $\boldsymbol{c_{MR}}$ denote the stiffness of the seat suspension system and the equivalent damping of the MR damper, respectively; and $\boldsymbol{z_1}$, $\boldsymbol{z_s}$, and $\boldsymbol{z_0}$ denote the displacement of the human body,

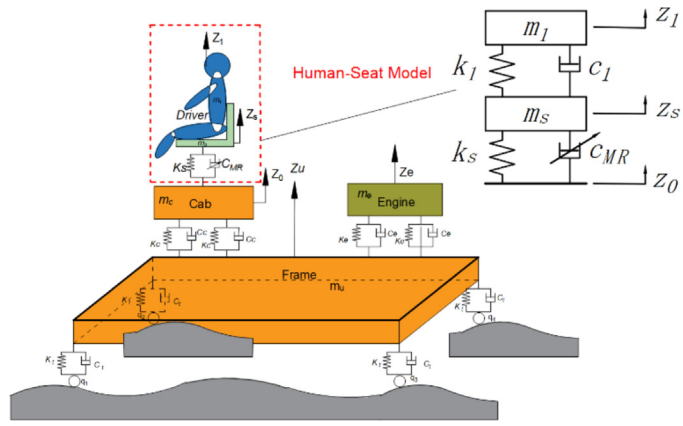

Fig. 1. 2-DOF "Human Seat" model.

the displacement of the seat, and the base input displacement excitation, respectively.

According to Newton's second law, the dynamics of the seat system is modeled as shown in equation (1).

$$\begin{cases} m_1\ddot{z}_1 + k_1(z_1 - z_s) + c_1(\dot{z}_1 - \dot{z}_s) = 0 \\ m_s\ddot{z}_s - k_1(z_1 - z_s) - c_1(\dot{z}_1 - \dot{z}_s) + k_s(z_s - z_0) + F_{MR} = 0 \end{cases} \tag{1}$$

Where, $\boldsymbol{F_{MR}}$ represents the damping force of the MR damper of the seat.

According to the modern control theory, equation (1) is rewritten into the state equation form as shown in equation (2).

$$\begin{cases} \dot{X} = AX + BU \\ Y = CX + DU \end{cases} \tag{2}$$

Where state variable $X=[z_1, z_s, \dot{z}_1, \dot{z}_s]^T$; input variable $U=[z_0, F_{MR}]^T$; output variable $Y=[z_1, z_s]^T$; The equation of state of the system after substitution is given by equation (3).

$$\dot{X} = \begin{bmatrix} 0 & 0 & 1 & 0 \\ 0 & 0 & 0 & 1 \\ -\dfrac{k_1}{m_1} & \dfrac{k_1}{m_1} & -\dfrac{c_1}{m_1} & \dfrac{c_1}{m_1} \\ \dfrac{k_1}{m_s} & -\dfrac{k_1 + k_s}{m_s} & \dfrac{c_1}{m_s} & -\dfrac{c_1}{m_s} \end{bmatrix} \begin{bmatrix} z_1 \\ z_s \\ \dot{z}_s \\ \dot{z}_1 \end{bmatrix} + \begin{bmatrix} 0 & 0 \\ 0 & 0 \\ 0 & 0 \\ \dfrac{k_s}{m_s} & -\dfrac{1}{m_s} \end{bmatrix} \begin{bmatrix} z_0 \\ F_{MR} \end{bmatrix} \tag{3}$$

$$Y = \begin{bmatrix} -\dfrac{k_1}{m_1} & \dfrac{k_1}{m_1} & -\dfrac{c_1}{m_1} & \dfrac{c_1}{m_1} \\ \dfrac{k_1}{m_s} & -\dfrac{k_1 + k_s}{m_s} & \dfrac{c_1}{m_s} & -\dfrac{c_1}{m_s} \end{bmatrix} \begin{bmatrix} z_1 \\ z_s \\ \dot{z}_s \\ \dot{z}_1 \end{bmatrix} + \begin{bmatrix} 0 & 0 \\ \dfrac{k_s}{m_s} & -\dfrac{1}{m_s} \end{bmatrix} \begin{bmatrix} z_0 \\ F_{MR} \end{bmatrix}$$

3 MR damper dynamics modeling

MR dampers are highly reliable, energy-efficient, controllable in output, and quick in response. However, their force-displacement and force-velocity characteristics are highly complex, exhibiting strong nonlinear features. As the control force calculated by the control algorithms must be output by the MR fluid damper, it is of the utmost importance to accurately comprehend the relationship between damping force, displacement, velocity, and current in order to guarantee precise control force output. This paper presents the results of mechanical characteristic tests conducted on MR dampers using an electrohydraulic servo fatigue testing machine, as illustrated in Figure 2. The test results were used to develop a forward dynamics model of the MR damper, which calculates the output damping force based on the relative motion displacement, velocity of the damper piston, and the input current.

3.1 Damping characteristics test of the MR damper

Damping force-velocity and damping force-displacement characteristic tests were conducted on MR dampers using an electro-hydraulic servo fatigue testing machine, as illustrated in Figure 2. The drive current was set from 0 to 1.5 A, with intervals of 0.5 A, piston relative speed from 0 to 1 m/s, speed intervals set at 0.05 m/s, and an amplitude of 29.2 mm. A sinusoidal signal with an amplitude of 10 mm and a frequency of 2 Hz was employed as the excitation. Tests were conducted on the MR damper within a drive current range of 0 to 1.5 A, with intervals of 0.5 A. The resulting force-velocity and force-displacement curves under excitation are presented in Figure 3.

3.2 The Bouc-Wen model of dampers

In order to ensure that the results of a system dynamics simulation are as close to reality as possible, it is necessary to establish a mathematical model that can accurately describe the mechanical characteristics of MR dampers. The Bouc-Wen model is an effective means of accurately representing the hysteresis characteristics of MR fluid dampers. It reflects the relationship between the damper and the piston's relative displacement and speed with greater accuracy than other models, which has led to its widespread use. The Bouc-Wen model is composed of a hysteresis system, springs, and viscous dampers in parallel, as illustrated in Figure 4.

The Bouc-Wen model is an effective approximation of the relationship between the output damping force of the MR fluid damper and the relative displacement and speed of the piston. The expression for the damping force is as follows:

$$\begin{cases} F_{MR} = c_{MR}\,\dot{x} + k_s(x - x_0) + \alpha z \\ \dot{z} = -\lambda|\,\dot{x}|z|z|^{n-1} - \beta\,\dot{x}|z|^n + Ax \end{cases}. \tag{4}$$

In the equation (4), $F_{M\,R}$ represents the damping force of the MR fluid damper, c_{MR} is the viscous damping coefficient, k_{s} is the stiffness coefficient, α is the proportion adjustment parameter of the hysteresis force in the damping force, and x_0 is the displacement offset from the relative equilibrium position. The hysteresis variable is represented by x, while v denotes the relative displacement and speed of the damper piston, respectively. The smoothness coefficient, n, is employed to adjust the model's smoothness and the linear characteristics of the curve from the pre-yield to the post-yield regions. Finally, the parameters γ, β, and A are utilized to adjust the model's smoothness and the linear characteristics of the curve from the pre-yield to the post-yield regions.

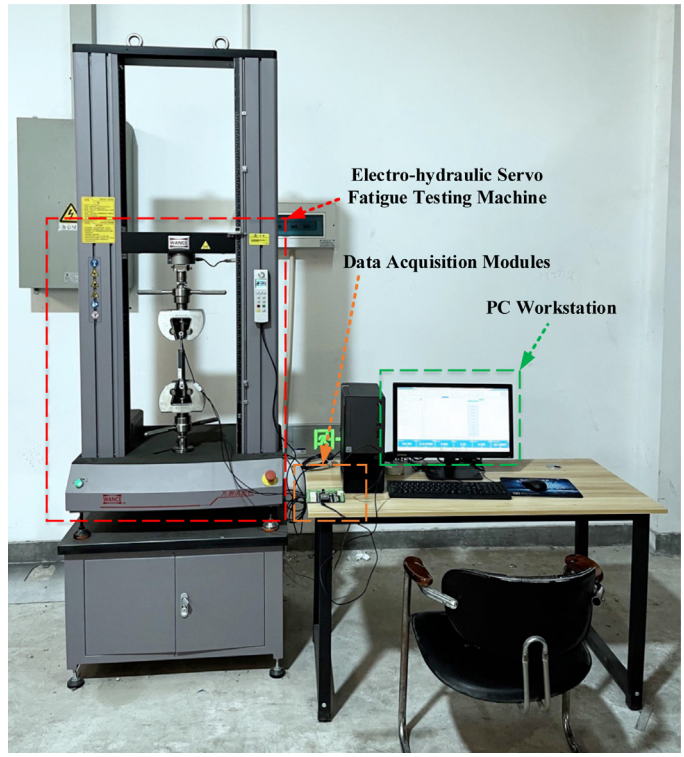

Fig. 2. 2 Damping characteristic test of the MR damper.

The Bouc-Wen model is constructed in Simulink and can be obtained from equation (4), as illustrated in Figure 5.

3.3 Modeling and parameter identification of MR dampers

The Bouc-Wen model is characterized by eight unknown parameters requiring systematic identification. While various optimization techniques such as GA and particle swarm optimization (PSO) have been widely adopted for parameter estimation, these methods are often limited by inherent complexity in their algorithmic implementation and significant computational demands. To address these challenges, this study employs the nonlinear least squares (NLS) method within the Simulink Design Optimization toolbox. The proposed approach utilizes an iterative optimization algorithm driven by experimental datasets to minimize the discrepancy between simulated and observed responses, thereby achieving high-fidelity parameter identification. Parameter identification is

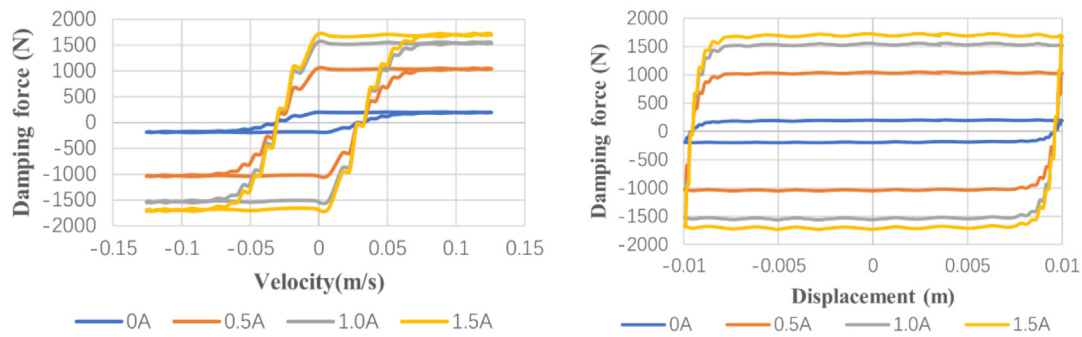

(a) Force-velocity curves for the MR damper (b) Force-displacement curve for the MR damper

Fig. 3. Force-velocity characteristics of the MR damper at different current levels and speeds.

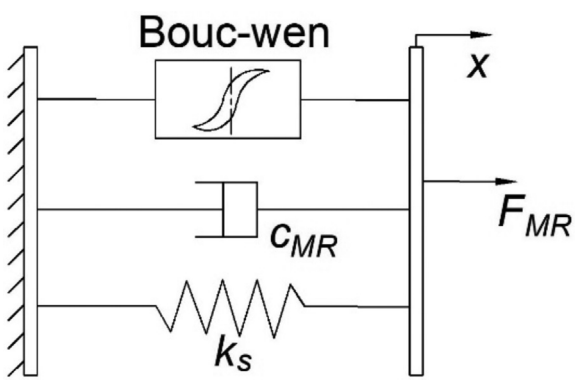

Fig. 4. Schematic diagram of the Bouc-Wen model structure.

accomplished by iteratively minimizing Q through gradient-based optimization. Comparative analysis demonstrates that the NLS method exhibits superior computational efficiency compared to metaheuristic algorithms like GA, while maintaining satisfactory accuracy (± 1.0% relative error in validation cases). The identified model is expressed mathematically as follows:

$$y = f(x', x'', \ldots, \theta', \theta'', \ldots) \tag{5}$$

Where y is the output of the system, x', x', ... is the input of the system; θ', θ', ... is the parameter. Once the parameters have been estimated, the mathematical expression of the model, f, is known, and the data are obtained experimentally as $(x_1', x_1'', \ldots, y_1)$, $(x_2', x_2'', \ldots, y_2)$, ...,$(x_n', x_n'', \ldots, y_n)$. The objective function Q, which represents the sum of squared errors for the nonlinear model, is defined as follows:

$$Q = \Sigma_{n=1}^{N}\left[y_n - f\left(x_n', x_n'', \ldots, \theta', \theta'', \ldots\right)\right]^2. \tag{6}$$

Eight unknown parameters in the Bouc-Wen model are identified by using the measured relative displacement, velocity, and current of the MR damper as inputs and the damping force as output. Once the Simulink modeling of the Bouc-Wen model was complete, the dynamic model parameters were identified through the use of experimental data obtained with an input excitation frequency of 2 Hz, an amplitude of 10 mm, and input currents of 0, 0.5 A, 1.0 A, and 1.5 A. The Bouc-Wen model comprises a total of eight unknown parameters, each of which exerts a distinct influence on the model. The preliminary identification of the model parameters revealed that there were significant changes in the values of α and c_0 with variations in current. Consequently, α and c_0 were designated to fluctuate in accordance with the operational conditions, whereas the remaining parameters were designated as constants. The fitting of the Bouc-Wen model revealed that the relationship between α, c_0, and current could be represented by a quadratic polynomial. The integration of the remaining six fixed parameters yields the parameter fitting results for the Bouc-Wen model, which are presented in Table 1.

Following the completion of the parameter identification process, the resulting data was graphed and compared with experimental results at an excitation frequency of 2 Hz and an amplitude of 10 mm, as illustrated in Figure 6.

Figure 6 depicts the experimental test results, represented by the solid line, and the model parameter fitting results, represented by the dashed line. As illustrated in Figure 6, the curve generated by parameter fitting using the Bouc-Wen model with Simulink parameter identification is in close alignment with the curve obtained from damper characteristic tests, indicating a high degree of fitting accuracy.

4 Control strategy design

This study begins with an examination of the control strategy, specifically the implementation of a semi-active control method for MR dampers. This method is designed to effectively attenuate the vibration response under low-frequency excitation, thereby enhancing the riding comfort of passengers. The control block diagram is depicted in Figure 7.

The concept of continuously adjustable intelligent control for MR dampers involves viewing the semi-active seat suspension system incorporating MR dampers as a whole nonlinear dynamic system. The control target is the seat suspension system of agricultural tractors. The monitoring of physical signals (including displacement, speed, and acceleration of the seat suspension) exhibited

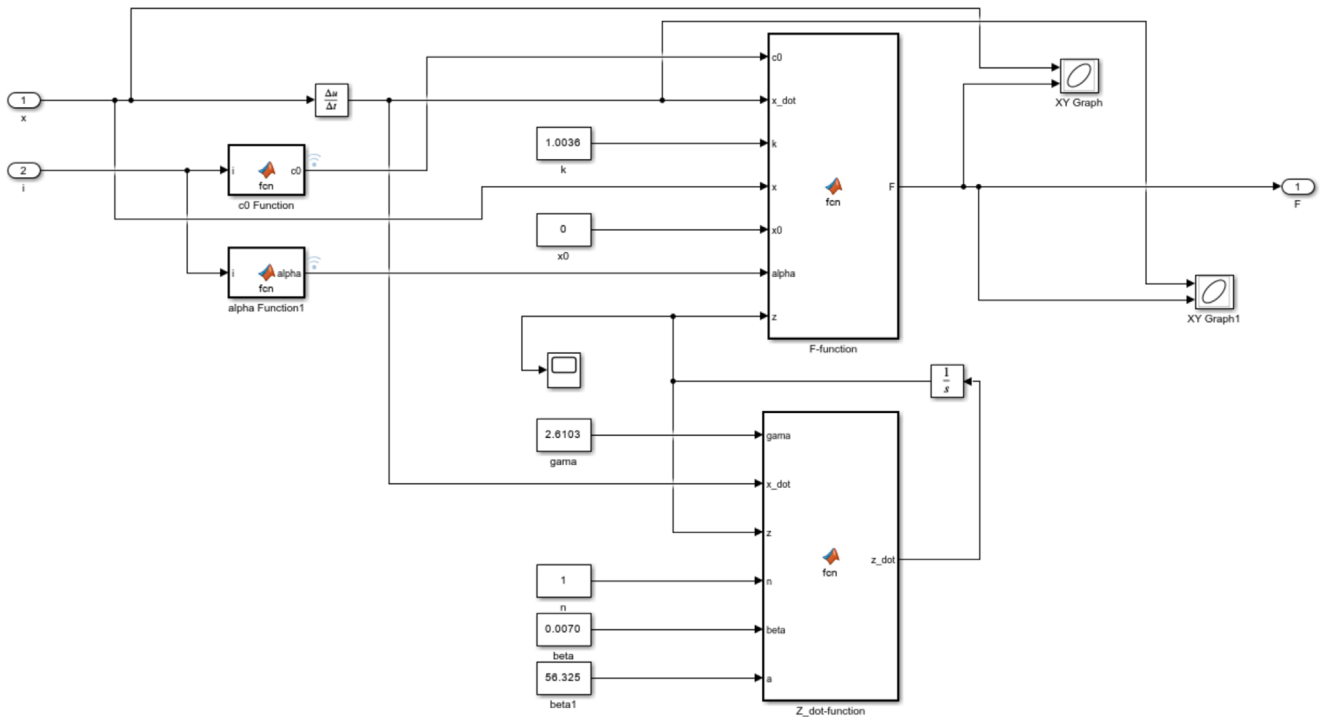

Fig. 5. Bouc-Wen simulation model.

Table 1. Bouc-Wen model parameters.

Parameters	Values
$c_{M\ R}$	0.0297 I^2+0.1621 I+0.1093
β	0.007
γ	2.72
n	1
k_s	1.004
x_0	0
A	55.237
α	$-31.75I^2$+93.58I+8.26

under road vibration excitation is followed by the data being fed into an MCU for processing. The ADRC control algorithm then outputs system control signals, specifically the working current of the MR damper coils, thus generating the corresponding damping controller. This structure is straightforward and effective, addressing all vibrations of the seat as external total disturbances. It employs closed-loop feedback to regulate the magnitude of the damping force, thereby reducing the impact of vibrations and enhancing seat comfort.

4.1 ADRC control strategy

The ADRC controller, as proposed by scholars such as Han Jingqing [19], is comprised of three primary components: a Tracking Differentiator (TD), an Extended State Observer (ESO), and Nonlinear State Error Feedback (NLSEF). The TD is employed primarily for the acquisition of differential signals and the configuration of transition processes. The ESO is utilized for the observation of total disturbances, while the NLSEF is responsible for the generation of control actions. The fundamental structure is depicted in Figure 8 below.

Given the nonlinear nature of NLSEF and the difficulty of analyzing it in practical applications, LADRC is often employed as a substitute in engineering projects. Gao Zhiqiang and others have further refined and optimized LADRC by employing linear gains instead of nonlinear gains, thereby streamlining the implementation and adjustment of the control algorithm [19–22]. The fundamental structure of the simplified LADRC is illustrated in Figure 9 below.

A review of the basic structure diagram of LADRC reveals that the functions of TD, LESO, and LSEF are interrelated, collectively facilitating effective control of the system. The desired dynamic behavior is defined by TD, while LESO provides real-time estimation of the system state. Based on this information, LSEF generates appropriate control signals, thereby achieving precise control of system dynamics. This method is particularly well-suited to systems with unknown or changing dynamics, as it does not require an accurate system model. The fundamental function of LADRC is to transform feedback acceleration data into excitation current control signals for MR dampers. This conversion process is of paramount importance in achieving precise control of the seat suspension system. During operation, an accelerometer is responsible for real-time monitoring of the displacement acceleration at the upper end of the suspension, and for the output of corresponding measurements. Subsequently, the aforementioned measurements are transmitted to the control subsystem, where they are compared with predetermined desired acceleration values. This comparison results in the

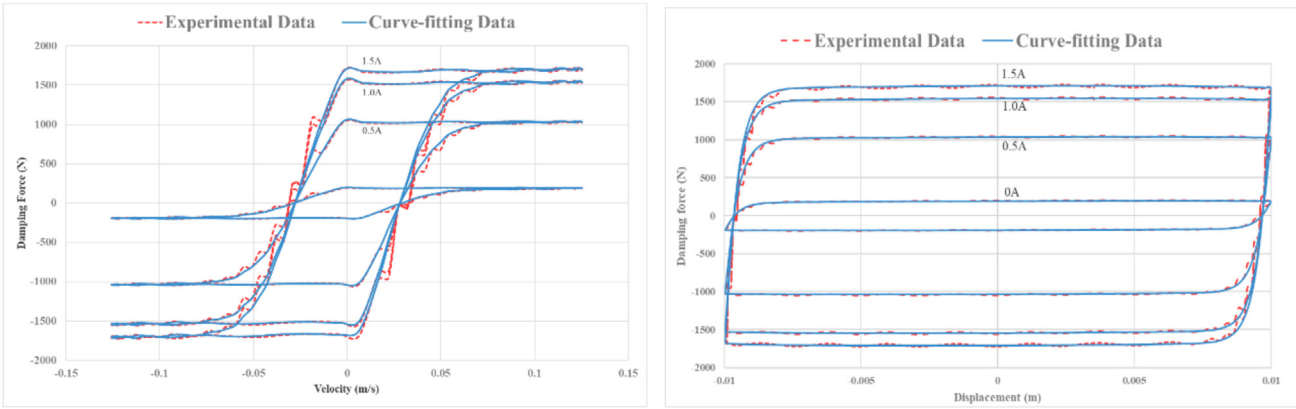

(a) 10mm，2Hz Force-velocity curve (b) 10mm，2Hz Force-displacement curve

Fig. 6. Results of damper model parameters and experimental results.

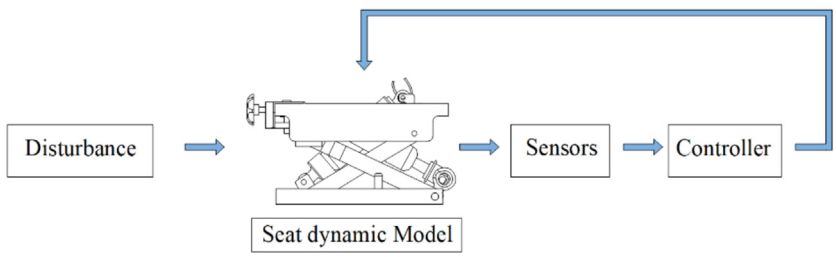

Fig. 7. Block diagram of two-degree-of-freedom seat suspension control.

generation of two deviation signals, designated e_1 and e_2, which represent the discrepancy between the actual and desired accelerations.

Although both ADRC and LADRC are robust control methods developed to handle unknown disturbances and model uncertainties, LADRC introduces linearization to simplify implementation. In classical ADRC, the Nonlinear State Error Feedback (NLSEF) component often poses tuning difficulties due to its nonlinearity. In contrast, LADRC replaces NLSEF with a Linear State Error Feedback (LSEF), significantly simplifying the design process while maintaining robustness. Given the computational constraints and the need for real-time response in agricultural machinery applications, LADRC was selected for this study. Its reduced parameter tuning complexity and superior real-time performance make it better suited for embedded systems where fast control loop execution is required.

The Linear State Error Feedback Control Laws employed by the LADRC permit real-time adjustment of the current in the seat suspension MR damper in response to deviation signals. MR dampers are a type of smart material whose damping characteristics can be adjusted by changing the size of the excitation current. In this manner, MR dampers are capable of adapting their damping force output in a manner that is responsive to the dynamic requirements of the suspension system. This adaptive adjustment mechanism enables the seat suspension system to more effectively absorb and reduce impacts and vibrations from the road, thereby providing a smoother and more comfortable riding experience.

4.2 LADRC controller design

From the two-degree-of-freedom human seat model (Eq. (1)):

$$\begin{cases} m_1\,\ddot{z}_1 = -k_1(z_1 - z_s) - c_1(\dot{z}_1 - \dot{z}_s) \\ m_s\ddot{z}_s = k_1(z_1 - z_s) + c_1(\dot{z}_1 - \dot{z}_s) - k_s(z_s - z_0) - F_{MR} \end{cases} \tag{7}$$

where m_1 represents the human body, k_1 and c_1 are constants.

By setting $F_b{=}{-}k_1(z_1{-}z_s){-}c_1(\dot{z}_1{-}\dot{z}_s)$ in equation (7), it transforms into a second-order model:

$$\ddot{z}_s = \frac{k_s z_0 - F_b - k_s z_s - F_{MR}}{m_s}. \tag{8}$$

Let $bu{=}{-}F_{MR}/m_s$, where b is the input gain, which is unknown, b_0 is the nominal value, and u is the input signal of the MR damper; let $y{=}z_s$ be the output of the MR damper; $a{=}k_s/m_s$ is a coefficient; $\omega{=}(k_s\ \ z_0{-}F_b)/m_s$ represents the external disturbance of the MR seat dynamic system. The final equation is simplified to the

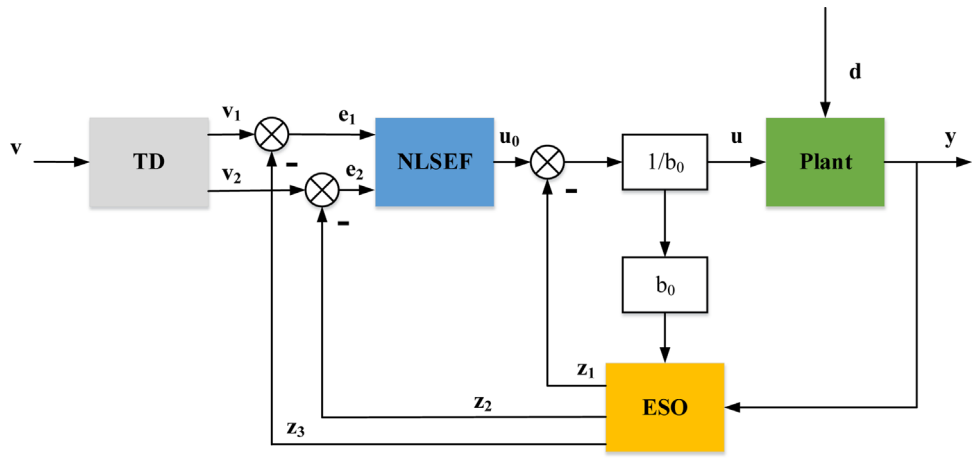

Fig. 8. ADRC basic structure diagram.

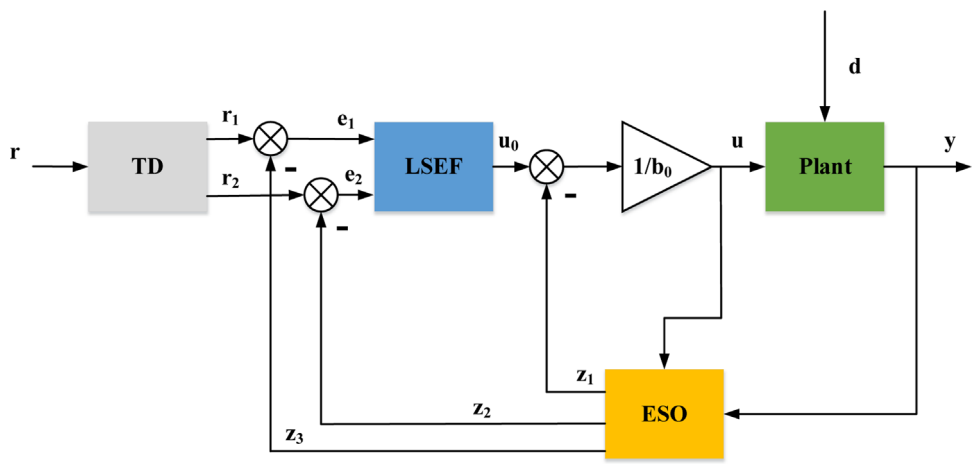

Fig. 9. Basic structure of LADRC.

following expression:

$$\ddot{y} = ay + \omega + bu. \tag{9}$$

One of the challenges associated with second-order LADRC is the design of a feedback controller that ensures the tracking of the reference input signal r. The nominal value b_0 is substituted for the true value b in the definition of the total disturbance, $f{=}a\ y{+}\omega{+}(b{-}b_0)\ u$. Subsequently, the introduction of state variables $x_1{=}y$, $x_2{=}\dot{y}$, and the extended state variable $x_3{=}\ f(y,\ \dot{y},\ w)$ allows for the rewriting of equation (9) as follows:

$$\begin{cases} \dot{x_1} = x_2 \\ \dot{x_2} = x_3 + b_0 u, y = x_1\ (10) \\ \dot{x_3} = h \end{cases} \tag{10}$$

Where x_1, x_2, x_3 are the system state variables, let $h{=}\dot{f}(y,\ \dot{f},\ \omega)$ and construct a linearly expanding state observer for equation (10).

$$\begin{cases} \dot{z_1} = z_2 - \beta_1(z_1 - y) \\ \dot{z_2} = z_3 - \beta_2(z_1 - y) + b_0 u\,. \\ \dot{z_3} = -\beta_3(z_1 - y) \end{cases} \tag{11}$$

By selecting an appropriate observer gain β_1, β_2 and β_3; the LESO is capable of achieving real-time tracking of each state variable within the system. By setting $u{=}(-z_3{+}u_0)/b_0$ and disregarding the estimation error of z_3 on $\dot{f}(y,\ \dot{y},\ \omega)$, the system can be simplified to a double-integrated series structure.

$$\ddot{y} = \Big[f(y, \dot{y}, \omega) - z_3\Big] + u_0 \approx u_0. \tag{12}$$

The objective is to design the PD controller:

$$u_0 = k_p(r - z_1) - k_d z_2. \tag{13}$$

Equation (13) where r is the reference signal and k_p, k_d is the controller gain, the core control law of LADRC, allows for real-time adjustments to the MR damper current based on the deviation between actual and desired acceleration. Under rough or shock road conditions, this deviation

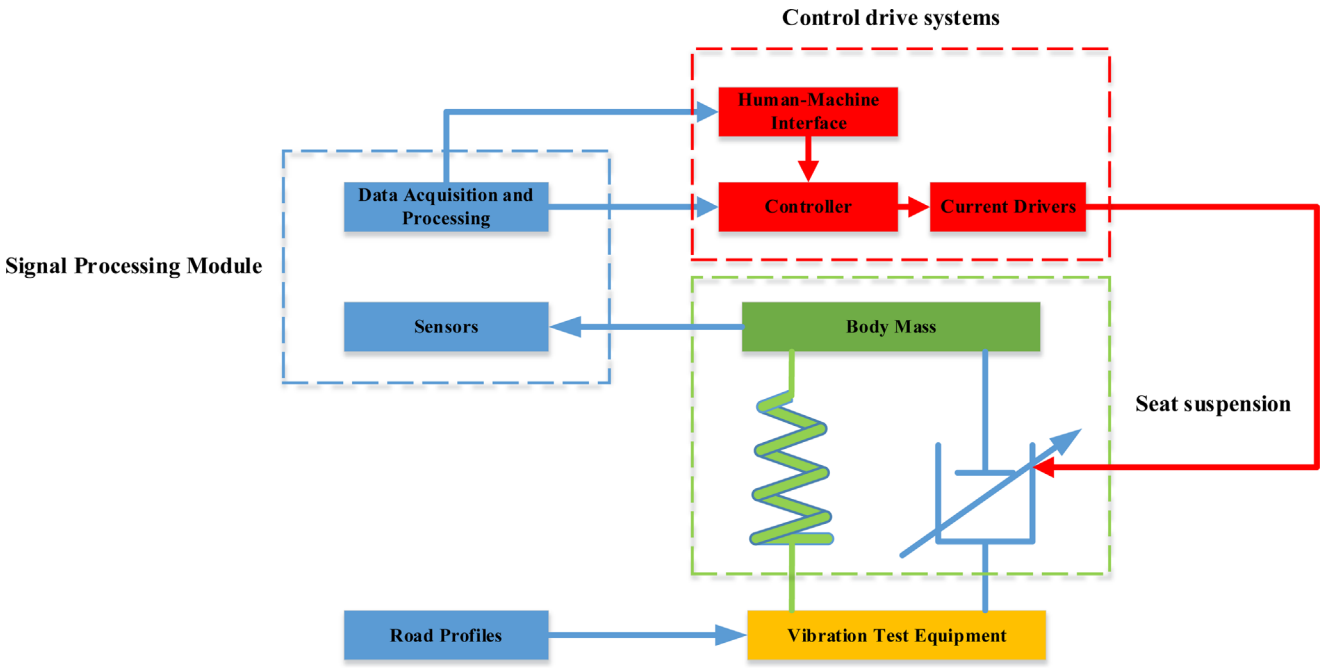

Fig. 10. Schematic diagram of the seat suspension vibration testing framework.

becomes more significant, prompting the controller to generate larger corrective actions through the increased current to the MR damper. This results in stronger damping force to suppress excessive vibration. Conversely, under smoother road profiles, the deviation is minimal, and the control law automatically reduces the actuation signal, preserving energy and reducing actuator wear. This adaptability enables LADRC to dynamically match road excitations without relying on explicit road condition classification or pre-trained models. According to equations (12) and (13) the system closed-loop transfer function can be obtained as follows:

$$G_{cl} = k_p/\left(s^2 + k_d s + k_p\right). \tag{14}$$

Moreover, the characteristic equation of LESO can be derived as follows:

$$\lambda(s) = s^3 + \beta_1 s^2 + \beta_2 s + \beta_3. \tag{15}$$

The selection of the optimal characteristic equation represents a pivotal stage in this process. This is demonstrated by the following equation:

$$\lambda(s) = (s + \omega_0)^3. \tag{16}$$

In equation (16), the observer bandwidth, denoted by ω_0, is used to derive the values of $\beta_1 = 3\omega_0$, $\beta_2 = 3\omega_0^2$, and $\beta_3 = \omega_0^3$.

In accordance with the literature (Gao), the parameters $k_p{=}{\omega_c}^2$ and $k_d{=}2\,\xi\,\omega_c$ are selected, with ω_c designated as the controller bandwidth and ξ as the damping ratio. This streamlines the configuration of LADRC controller parameters, necessitating only the selection of the observer bandwidth ω_0 and controller bandwidth ω_c. By configuring reasonable values for b_0, ω_0, and ω_c in the LADRC controller, the desired performance of the seat vibration dynamic control system can be achieved.

From a practical implementation perspective, LADRC has proven to be suitable for real-time control applications due to its relatively low computational load. Compared with nonlinear or model-predictive control algorithms, LADRC's reliance on linear feedback and observer structures allows it to be implemented on low-power microcontrollers such as STM32 or DSPs commonly used in vehicle systems [23–25]. The controller structure, involving only a few gains and a second-order observer, ensures that computation remains within acceptable time bounds for real-time damping control, even under rapid excitation changes.

5 Seat suspension simulation analysis

A seat suspension vibration testing framework was constructed in order to simulate the vibration of the seat suspension within the cabin of an agricultural tractors, as illustrated in Figure 10. A vibration table was employed to output road unevenness excitation signals, which were then transmitted to the seat suspension system. The signal processing system collected acceleration, displacement, and other signals from the seat suspension system sensors, which were subsequently subjected to data preprocessing before being transmitted to the controller and the human-machine interface. At this stage, the severity of seat vibrations could be analyzed and assessed offline. The controller generates control signals for the current driver of the MR damper, based on real-time sensor data and a pre-designed control strategy. This results in the generation of a damping force acting on the seat suspension system,

Table 2. Main parameters of the seat suspension system for agricultural tractors, including damping coefficients and stiffness.

values.

Parameters	Values	Parameters	Values
m_1	80 kg	k_1	105000 N/m
m_s	10 kg	k_s	12350 N/m
c_1	550 N · s/m		

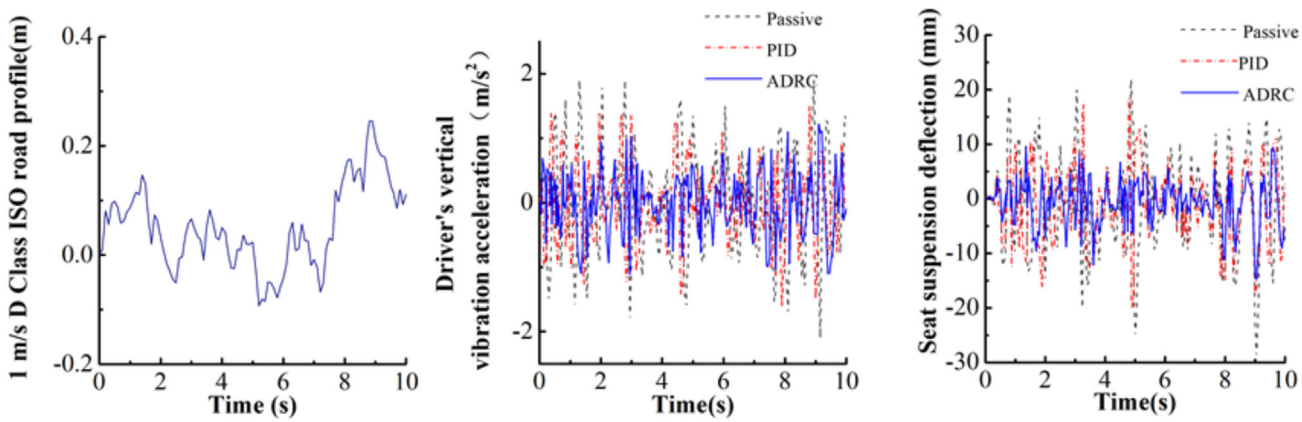

Fig. 11. Simulation of Class D road profile at 1 m/s.

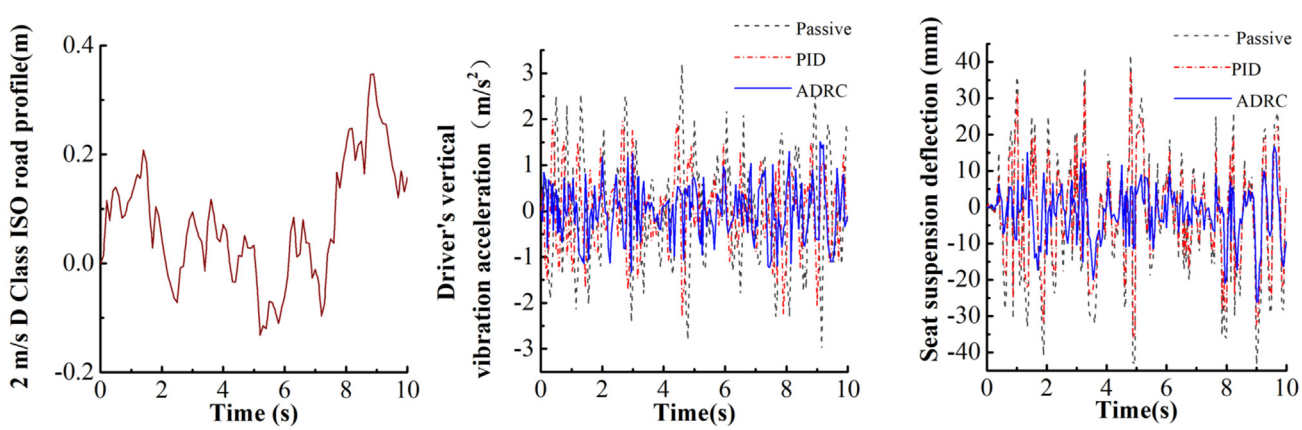

Fig. 12. Simulation of Class D road profile at 2 m/s.

thereby achieving active vibration isolation of the seat suspension.

To ascertain the efficacy of the MR damper in the seat suspension, the designed LADRC control was subjected to comparison with passive and PID controls. The simulation conditions assumed that agricultural equipment traveled at speeds of 1 m/s and 2 m/s on an ISO Class D road profile, with road excitation that considered both random and shock road conditions. Table 2 presents the parameters of the seat suspension system, including springs and dampers, along with the corresponding simulation results.

Figures 11–14 illustrate the simulation outcomes for the vertical vibration acceleration and dynamic travel of the seat suspension in agricultural machinery. The figures demonstrate that, in comparison to passive and PID controls, LADRC enhances the vibration isolation performance of the cabin suspension system to a greater extent. To facilitate a more comprehensive understanding of the performance advantages of LADRC in seat suspension, the root mean square values of relevant suspension performance indicators are also presented in Table 3. As illustrated in Table 3, the root mean square values of the vertical vibration acceleration with LADRC are reduced to varying degrees in comparison to the other two types of suspension. In terms of the dynamic travel of the seat suspension, the dynamic travel of the LADRC suspension system decreased significantly compared to both the PID suspension and the passive suspension at 1 m/s and 2 m/s, respectively. Furthermore, the performance was also good in both shocked and unshocked conditions. The enhancement of external shock disturbances did not lead to a significant increase in the dynamic

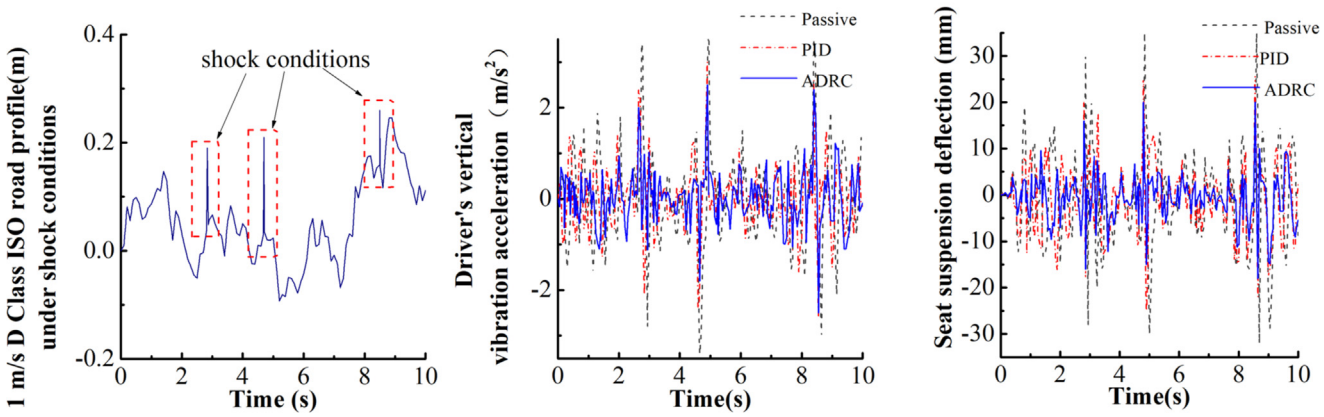

Fig. 13. Simulation of Class D road profile at 1 m/s under shock conditions.

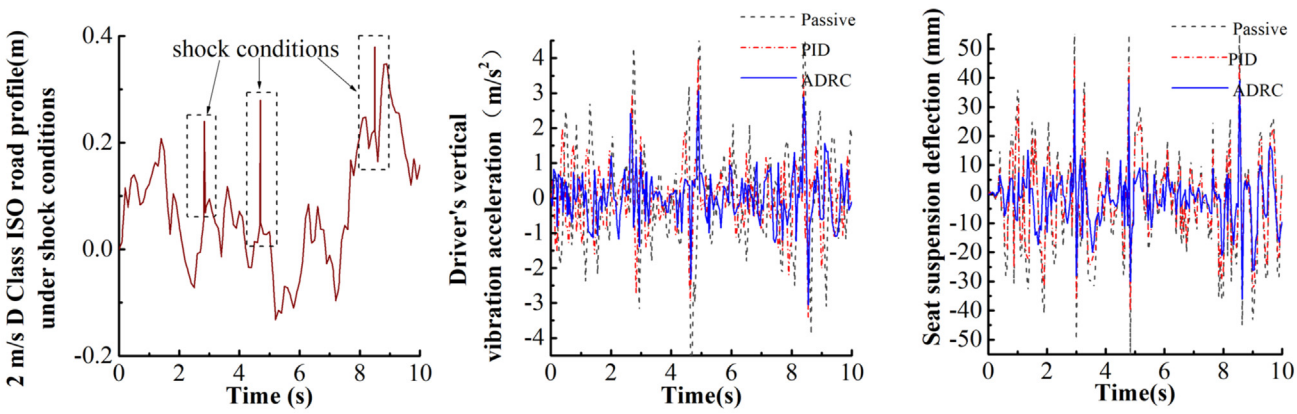

Fig. 14. Simulation of Class D road profile at 2 m/s under shock conditions.

Table 3. Simulation comparison of seat suspension control performance.

Speed	Simulation results	Passive	PID	LADRC
1 m/s	a_v	0.816	0.727	0.618
	a_s	0.880	0.766	0.666
2 m/s	a_v	0.974	0.845	0.687
	a_s	1.050	0.884	0.741

travel of the seat, which also reflects the robustness of the ADRC control strategy.

Under ISO Class D road excitation conditions, the LADRC performance was evaluated in extreme operational scenarios illustrated in Figures 13 and 14, including abrupt road amplitude escalation (200% of nominal excitation amplitude). The controller maintained stable vibration suppression without control divergence or error propagation, confirming its operational robustness under critical disturbance conditions.

As demonstrated in Table 3, where a_v is the Driver's vertical vibration acceleration (D class road profile without shock) and a_s is the Driver's vertical vibration acceleration (D class road profile under shock conditions). The RMS values of vertical vibration acceleration of the ADRC suspension system decreased by 15.0% and 24.2% in comparison to the PID suspension and the passive suspension, respectively, at a speed of 1 m/s in the absence of shock conditions. At a speed of 2 m/s, the decreases were 18.7% and 29.5%, respectively, and the ADRC seat suspension system demonstrated satisfactory performance at different speeds. Moreover, the RMS values of vertical vibration acceleration of the ADRC suspension system decreased by 13.1% and 24.3% under shock conditions at 1 m/s, and by 16.2% and 29.4% at 2 m/s, respectively. The reduction in RMS vertical acceleration by 15.0% and 24.2% at 1 m/s, and by 18.7% and 29.5% at 2 m/s, indicates a significant reduction in seat vibration. This translates directly into improved operator comfort, as lower RMS values are strongly correlated with less perceived vibration, which is a major factor in reducing operator fatigue. The reduced vibration exposure lowers the risk of

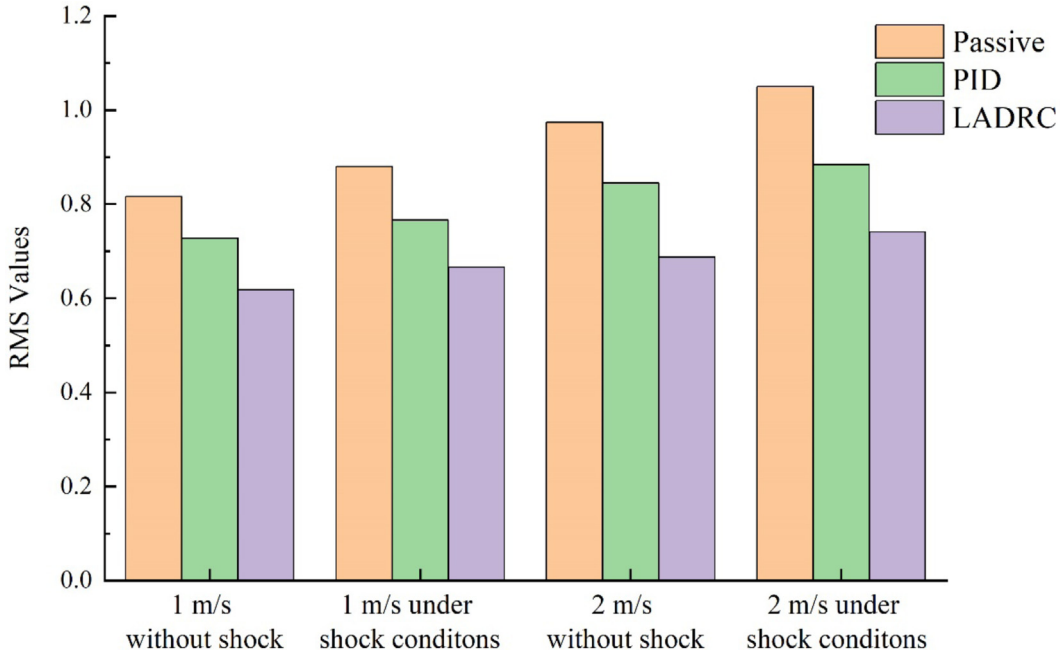

Fig. 15. Comparison of RMS Vertical Acceleration under Different Control Strategies and Speeds.

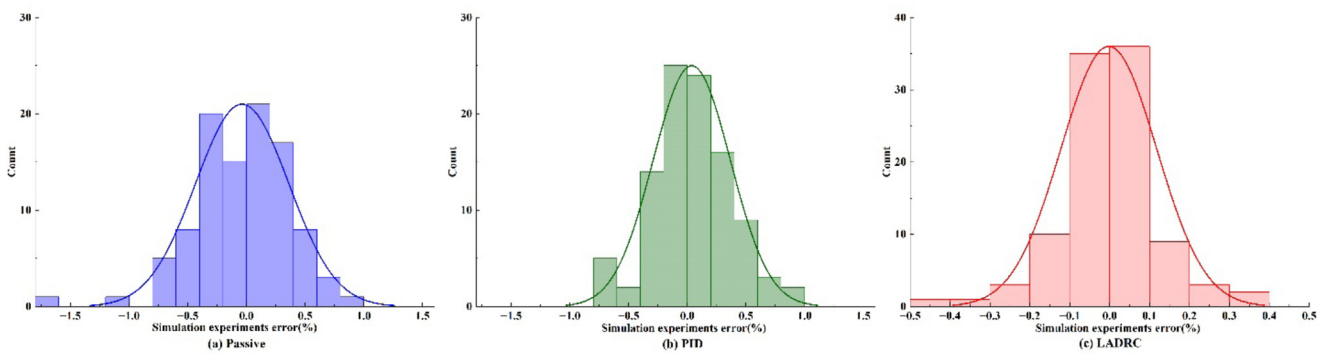

Fig. 16. Error probability distribution curves of different control strategies.

musculoskeletal disorders and enhances the operator's ability to work for longer periods without discomfort, ultimately increasing operational efficiency. Figure 15 shows the comparison of RMS vertical acceleration under different speeds and control strategies. The increase in external shock disturbances did not result in a decline in controller performance, which indicates the resilience of the ADRC control strategy. In addition to enhancing operator comfort, the use of LADRC contributes to long-term cost savings by reducing the wear on suspension components. The precise control of the MR damper, which minimizes excessive movement and impact forces, directly leads to less stress on the suspension system. This results in a reduced need for maintenance and fewer component replacements, thereby lowering the overall operational costs for agricultural machinery.

In order to verify the stability of the LADRC control strategy, simulation experiments with small changes in initial conditions and system parameters were carried out under extreme conditions or uncertain parameters (sensor noise and ± 10% variation in damping gain were added). A total of 100 simulation data sets were collected and the error probability distribution curve was plotted (as shown in Fig. 16). The results show that the error distribution of the LADRC method is the most concentrated, and the probability density peak is near zero, showing reliable performance, robustness and effective anti-interference ability.

The modeling in this study assumes linearity within certain dynamic ranges, particularly when estimating the damping force of the MR damper. While this assumption simplifies the modeling process and is suitable for most operating conditions, it may not fully capture the complex nonlinear behavior of MR fluids under extreme conditions. Future work may involve incorporating more detailed models to account for these nonlinearities, especially under high-frequency or large-amplitude excitation, which may be encountered in more demanding operational environments. The energy-efficient nature of MR dampers not only contributes to improved operational performance but also

has potential environmental benefits. By reducing the need for frequent maintenance and component replacements, the lifespan of the suspension system is extended, reducing the overall environmental impact associated with manufacturing and waste disposal of components. Furthermore, the efficient energy use in damping control helps minimize the carbon footprint of agricultural operations.

6 Conclusion

In this paper, we first present the results of a mechanical properties test on a MR damper. Based on these results, we establish a Bouc-Wen nonlinear model of the MR damper. We then fit the model parameters to the current using the least-squares method, deriving an accurate mathematical equation for the model parameters in relation to the current. This accurately describes the mechanical behavior of the MR damper. Secondly, a LADRC strategy is designed for the two-degree-of-freedom suspension model of the agricultural machine seat. This control strategy is capable of achieving effective control of the semi-active seat suspension system. Finally, a simulation analysis was conducted to assess the performance of the designed LADRC control algorithm in comparison to PID control and passive control. The results demonstrated that the LADRC algorithm exhibited superior vibration damping performance in Class D road excitation under different operating conditions, effectively controlling the damped continuously adjustable seat suspension. Looking forward, the integration of AI-driven optimization algorithms could enhance the tuning process for the LADRC parameters, allowing for real-time adjustment based on changing operational conditions. Machine learning techniques such as reinforcement learning could be employed to continuously adapt the control parameters, improving system efficiency and robustness in dynamic environments.

In addition to agricultural tractors, the LADRC-based MR damper suspension system could be applicable to a wide range of agricultural machinery and industrial vehicles, such as forklifts, harvesters, and excavators. The adaptability of the LADRC controller to different operational environments and machinery types suggests that it could play a significant role in improving ride comfort and system longevity across various industrial sectors.

Funding

This research was funded by the Natural Science Foundation of Fujian Province (grant nos. 2022J011191 and 2024J01909), the Fujian Provincial Key Science and Technology Project: Key Technologies and Equipment for Continuous and Intelligent Production of Bamboo Scrimber (grant no. 2024HZ026011), the Nanping Science and Technology Plan Project (grant nos. N2023Z001, N2023Z002, N2023J001 and N2024Z001) and horizontal projects of Wuyi University (grant no. 2024-WHFW030).

Conflicts of interest

The contact author has declared that none of the authors has any competing interests.

Data availability statement

The datasets used and/or analyzed during the current study are available from the corresponding author on reasonable request.

Author contribution statement

Bin Chen and Bo Guo discussed and decided on the methodology of the study and prepared the paper. Zhou Luyang and Zheng Zhixiong contributed to the prototype and test. Wu Jianjin and Duan Minghao contributed to the model building.

References

[1] Q. Jiang, W. Ni, X. Zhang, P. Chen, L. Xu, Y.J.P.o.t.I.o.M. E. Yang, Evaluation of tractor driving comfort according to the steering angle and speed using a virtual prototype, Part D: J. Autom. Eng. **235**, 1191–1199 (2021)

[2] K.P. Lanças, A.C. Marques Filho, M.d.S. Moura, F.A.d.J. Damasceno, D.R.J.R.C.A. Balestrin, Agricultural tractor test, **51**, e20207750 (2020)

[3] A. Singh, N. Nawayseh, H. Singh, Y.K. Dhabi, S.J.E.A.o.A.I. Samuel, Internet of agriculture: analyzing and predicting tractor ride comfort through supervised machine learning, **125**, 106720 (2023)

[4] K. Choi, J. Oh, H.-S. Kim, H.-W. Han, J.-H. Park, G.-H. Lee, J. Seo, Y.-J.J.A.S. Park, Experimental study on the dynamic characteristics of hydro-pneumatic semi-active suspensions for agricultural tractor cabins, **10**, 8992 (2020)

[5] A. Soliman, M.J.J.o.L.F.N. Kaldas, Vibration, A. Control, Semi-active suspension systems from research to mass-market A review, **40**, 1005–1023 (2021)

[6] M. Watanabe, K. Kazama, K. Sakai, Development of nonlinear bouncing tractor model with semi-active axle suspension system, 2023 ASABE Annual International Meeting, American Society of Agricultural and Biological Engineers, 2023, pp. 1

[7] H. Gheibollahi, M. Masih-Tehrani, A. Najafi, Improving ride comfort approach by fuzzy and genetic-based PID controller in active seat suspension, Int. J. Autom. Control. **18**, 184–213 (2024)

[8] S.K. Sharma, R.C. Sharma, J. Lee, Modelling and simulation of MR damper characterization and uncertainty assessment in marine engine vibration isolation with FLPID control, Int. J. Modell. Simul. **1-11** (2024)

[9] H. Gheibollahi, M. Masih-Tehrani, A multi-objective optimization method based on NSGA-II algorithm and entropy weighted TOPSIS for fuzzy active seat suspension of articulated truck semi-trailer, Proc. Inst. Mech. Eng. Part C: J. Mech. Eng. Sci. **237**, 3809–3826 (2023)

[10] A. Najafi, M. Masih-Tehrani, A. Emami, M. Esfahanian, A modern multidimensional fuzzy sliding mode controller for a series active variable geometry suspension, J. Braz. Soc. Mech. Sci. Eng. **44**, 425 (2022)

[11] A.D. Damavandi, M. Masih-Tehrani, B. Mashadi, Configuration development and optimization of hydraulically interconnected suspension for handling and ride enhancement, Proc. Inst. Mech. Eng. Part D: J. Autom. Eng. **236**, 381–394 (2022)
[12] J. Kim, T. Lee, C.-J. Kim, K. Yi, Model predictive control of a semi-active suspension with a shift delay compensation using preview road information, Control Eng. Pract. **137**, 105584 (2023)
[13] G. Li, Z. Ruan, R. Gu, G. Hu, Fuzzy sliding mode control of vehicle magnetorheological semi-active air suspension, **11**, 10925 (2021)
[14] Z. Gao, P.K. Wong, J. Zhao, X. Hua, X. Ma, Z.J.A.M.M. Xie, Design of compensatory backstepping controller for nonlinear magnetorheological dampers, **114**, 318–337 (2023)
[15] W. Jun, L. Yunfei, Q. Zhaoye, M. Liang, C.J.C.J.o.A. Fulei, Nonlinear characteristic investigation of magnetorheological damper-rotor system with local nonlinearity, **36**, 111–126 (2023)
[16] M.B. Kumbhar, R.G. Desavale, S.G.J.A.J.f.S. Kumbhar, Engineering, dynamic characterization of MR fluid-based dynamic vibration absorber, **48**, 11363–11377 (2023)
[17] J. Peng, L. Wang, Y. Zhao, S.J.N.D. Lenci, Time-delay dynamics of the MR damper-cable system with one-to-one internal resonances, **105**, 1343–1356 (2021)
[18] J. Yang, D. Ning, S. Sun, J. Zheng, H. Lu, M. Nakano, S. Zhang, H. Du, W.J.M.S. Li, S. Processing, A semi-active suspension using a magnetorheological damper with nonlinear negative-stiffness component, **147**, 107071 (2021)
[19] J. Han, From PID to active disturbance rejection control, IEEE Trans. Ind. Electron. **56**, 900–906 (2009)
[20] C. Dai, Z. Gao, Y. Chen, D.J.P. Li, Generalized conditional feedback system with model uncertainty, **12**, 65 (2023)
[21] H. Jin, Z.J.C.T. Gao, Technology, on the notions of normality, locality, and operational stability in ADRC, **21**, 97–109 (2023)
[22] S. Liu, Z. Gao, Y. Chen, Y. Wang, D. Li, M.J.J.o.E.S. Zhu, Enhancing process state monitoring in energy storage systems: A robust design synthesis with physics-informed generalized observer, **87**, 111391 (2024)
[23] C. Zhu, Y. Jiang, D. Shen, Y. Zhao, Research on the temperature control of a cryogenic urine storage system based on improved adaptive LADRC, J. Phys.: Conf. Ser. (1), IOP Publishing, 2024, pp. 012023
[24] X. Zhao, P. Tian, H. Zhang, H. Wu, X. Ye, L. Zhang, F. Zhao, J. Sun, Rotation measurement system based on linear active disturbance rejection and quasi-proportional resonant control, Measurement. **244**, 116306 (2025)
[25] X. Hou, Y. Ma, C. Xiang, Steering control of electric tracked vehicle based on second-order disturbance observer and multi-objective optimization, Proc. Inst. Mech. Eng. Part D: J. Autom. Eng. 09544070241246046 (2024)

Cite this article as: B. Chen, B. Guo, L. Zhou, Z. Zheng, J. Wu, M. Duan, Agricultural tractors magneto-rheological seat suspension design based on LADRC control strategy, Mechanics & Industry **26**, 35 (2025), https://doi.org/10.1051/meca/2025017